Am J Cancer Res 2021;11(12):5979-5991
www.ajcr.us /ISSN:2156-6976/ajcr0138533

Original Article

Establishment and validation of an autophagy-related prognostic signature for survival predicting in cutaneous melanoma

Hongjun Fei, Xiongming Chen

Department of Reproductive Genetics, International Peace Maternity and Child Health Hospital, Shanghai Key Laboratory of Embryo Original Diseases, Shanghai Municipal Key Clinical Specialty, Shanghai Jiao Tong University School of Medicine, Shanghai 200030, China

Received August 24, 2021; Accepted October 21, 2021; Epub December 15, 2021; Published December 30, 2021

Abstract: Existing staging system for prognosis evaluating for Skin Cutaneous Melanoma (SKCM) patients had defects of subjective, inaccuracy and inconsistently, therefore, to identify specific and applicable prognostic markers and promote personalized therapeutic interventions is urgently required. This study aims to build a robust autophagy-related genes (ARGs) signature for prognosis monitoring of SKCM patients. We determined 26 ARGs as differentially expressed autophagy-related genes (DEARGs) from 103 SKCM and 23 normal skin samples in GSE15605 and GSE3189 datasets. Optimal prognostic DEARGs composed the risk model were screened and verified in 458 SKCM patients in TCGA cohort as the training cohort and 209 patients in GSE65904 as the test cohort. Finally, 4 optimal independent prognostic DEARGs (*CAPNS1*, *DAPK2*, *PARP1* and *PTK6*) were filtered out in the training cohort to establish the risk model. A prognostic nomogram was established for quantitative survival prediction. The risk model grouped high-risk SKCM cancer patients exhibited significantly shorter survival times in both training and test cohorts. The area under the ROC curve for risk score model was 0.788 and 0.627 in the training and test cohorts indicated the risk model was relatively accurate for prognosis monitoring. Clinical correlation analysis exhibited that risk score was an independent predictor for prognosis significantly associated with T/N classification. The prognostic value of the 4 risk genes formed the risk model was also validated respectively. We identified a novel autophagy-related signature for prognosis monitoring. It has the potential to be an independent prognostic indicator and can benefit targeted therapy.

Keywords: Skin cutaneous melanoma, autophagy-related genes, prognostic risk model, targeted therapeutic intervention, survival prediction

Introduction

As per the GLOBOCAN, the number of new cancer cases and deaths from cancer are expected to be 19.3 million and 10 million in 2020 worldwide [1]. Skin Cutaneous Melanoma (SKCM) is one of the most lethal malignant tumors of the skin, it leads to more than 90% of skin cancer-related deaths [2, 3]. According to reports from the American Cancer Society, about 7,180 people died of Skin Cutaneous Melanoma (SKCM), and about 106,110 new cases are diagnosed in 2021 in the US. Melanoma is more common in males than females [4]. Local melanoma is usually curable by adequate surgery, the 5-year survival rate for patients with local melanoma and treated early is 95% to 99% [5]. However, SKCM is more likely to spread than other skin cancers: after primary tumor excision, about 1/3 of the patients developed metastasis in various organs [6]. The 5-year survival rate for patients with melanoma that metastasized to distant tissues is only 5% to 19% [7]. Since the prognosis of advanced SKCM is poor, there has been an emphasis on early diagnosis and the need for better therapeutic strategies at an earlier stage of disease [8].

Traditionally, the American Joint Committee on Cancer (AJCC) Staging was used to evaluate the risk of tumor recurrence for SKCM [9, 10],

Table 1. Characteristic of microarray data that used to do difference analysis

Expression profiling array (Skin & SKCM)	Platforms	GEO accession	Samples
Genome	GPL570	GSE15605	16 Skin; 58 SKCM
Genome	GPL96	GSE3189	7 Skin; 45 SKCM

it was a powerful tool for evaluating patient prognosis and making a treatment plan, and may be helpful for recovery or prolonged survival of patients [11-13], but widespread reports showed that, despite an international staging system, the diagnosis and prognostic prediction of SKCM were still difficult to render consistently and accurately [14-16]. Therefore, it is significant to develop novel and specific prognostic biomarkers for risk stratification and treatment optimization in SKCM patients. The specific and applicable biomarker may shed light on the guidance of personalized therapeutic interventions and new therapeutic target development.

Autophagy is a non-specific intracellular degradation system that can break down and clean internally superfluous proteins in cells, finally, cellular components are recycling [17]. Autophagy-Related Genes (ARGs) are key players in autophagy. Multiple reports demonstrated that autophagy is associated with SKCM progression. For example, pre-clinical models and clinical trials demonstrated that decreased autophagic activity in SKCM improved the efficacy for therapy [18, 19]. Nevertheless, there is no prior study that assessed the autophagy effect on SKCM prognosis through large-scale expression patterns. Hence, the purpose of our study is to construct a prognostic risk signature for SKCM patients employing ARGs. In our report, the association between expression profiles of differentially expressed autophagy-related genes (DEARGs) and clinical indicators were examined in 458 SKCM patients and constructed a risk prognostic model as an independent predictor for survival status and survival time through ARGs. Multiple validation analysis results evidently support our prognostic risk model. The novel risk prognostic model will be of great benefit to risk stratification and treatment optimization in SKCM patients, the specific DEARGs that formed the risk prognostic model can provide new directions of personalized therapeutic interventions and new therapeutic target development.

Methods

Data acquisition

The gene expression profiling data sets (ID: GSE15605, GSE3189) and survival data sets (ID: GSE65904) were obtained from the Gene Expression Omnibus database (https://www.ncbi.nlm.nih.gov/geo/). The brief information of 2 GEO datasets (ID: GSE15605, GSE3189) from 2 independent laboratories which were used to analyses group differences [containing 23 human normal skin and 103 Skin cutaneous melanoma (SKCM) specimens] were extracted and listed in **Table 1**. The survival data of 209 SKCM patients from GSE65904 was used as a test group to verify our autophagy-related risk model. The transcript sequencing data and the associated clinical information of 458 SKCM patients that were used as training group to construct and verify the autophagy-related prognostic risk signature were obtained from TCGA database (https://portal.gdc.cancer.gov/). There are 232 genes that were considered autophagy-related genes (ARGs) so far were obtained from the Human Autophagy Database (HADb).

Identification and functional analysis of differentially expressed autophagy-related genes (DEARGs)

The expression profiling data in 2 independent GEO datasets GSE15605 and GSE3189 were batch normalized to eliminate the systematic differences by R software. There are 103 SKCM tissues and 23 skin tissues totally in the 2 GEO datasets. The differential analysis of autophagy-related genes (ARGs) between SKCM and normal tissues was done by the "limma" package in R with filter criteria of $|\log_2\text{Fold Change}|$ ($|\log_2\text{FC}|$) >1 and adjusted *P*-value <0.05.

For exploring the key roles of all identified DEARGs, Gene Ontology (GO) functional annotation and Kyoto Encyclopedia of Genes and Genomes (KEGG) pathway enrichment analyze were performed by "ClusterProfiler" and "ggplot2" packages in R. For understanding the relationship among identified DEARGs, we constructed and visualized a protein-protein interaction (PPI) network for all DEARGs by STRING database (https://string-db.org/) and Cytoscape software respectively.

Construction of survival-related risk prognostic model

The TCGA-Skin Cutaneous Melanoma (SKCM) cohort was the training set to construct and verify the prognostic model. The prognostic value of all DEARGs in 458 SKCM patients of the TCGA cohort was computed by a univariate Cox proportional hazards analysis, the survival-related DEARGs were identified with the threshold of $P<0.05$. Then we carried out the multivariate Cox regression analysis based on prognostic DEARGs obtained from univariate Cox analysis to structure the prognostic predictive model in the training set. At this point, we obtained several optimal risk DEARGs that formed the model and their respective coefficients value according to the training cohort. The risk score for every SKCM patient was added up by the expression values of all risk DEARGs multiplied by their regression coefficients. The formula was: risk score = $\sum_{i=1,2,...,n}$ regression coefficient (genei) × expression value of (genei). Through the formula, the risk score of each SKCM patient was calculated in the training cohort and test cohort respectively, and SKCM patients were divided into a high-risk group and a low-risk group according to the median risk score obtained in the training cohort as the division. Finally, a nomogram based on identified risk DEARGs was constructed by the "rms" R package for a quantitative prediction tool for prognosis evaluation.

Validation the performance of OS risk prognostic model in training cohort and external cohort

The GSE65904 cohort containing clinical information of 209 SKCM patients was an external cohort that was used as the test cohort. The performance of the prognostic risk model was verified in the training cohort and test cohort respectively. The survival curves were generated by the "survival" R package and assessed the differences in survival between the high-risk group and low-risk group. The areas under the curve (AUC) of the receiver operating characteristic (ROC) curve of multiple clinicopathological indicators and risk score to check the accuracy of the prognostic model were constructed with the R package of "survivalROC". The larger the AUC, the better the performance of the clinical parameter to predict prognosis. We also visualized the correspondence between the survival status of SKCM patients and risk scores.

To test whether the risk prognostic model could be independent of traditional clinical characteristics as a novel prognostic indicator, the "beeswarm" R package was used to perform Cox regression analyses. Clinical characteristics of SKCM patients including age, gender, pathological stage, and T/N/M classification were collected from the training cohort and integrated with the risk score of each patient for further correlation analysis.

The prognostic value of four risk DEARGs that composed the risk model

Kaplan-Meier survival curves were drawn with the R package to compare survival differences of diverse expressions for 4 risk DEARGs (*CAPNS1*, *DAPK2*, *PARP1* and *PTK6*) respectively. The expression difference of 4 risk DEARGs on mRNA and protein level between SKCM and control tissues was verified in Oncomine Database (https://www.oncomine.org) and The Human Protein Atlas (http://www.proteinatlas.org).

Single-gene gene set enrichment analysis (GSEA) on 4 prognostic-related DEARGs

To explore which pathways were active when different expressions of 4 risk DEARGs, GSEA analysis of 4 risk DEARGs was performed using c2.cp.kegg.v7.0 annotated set. Firstly, an ordered list of all genes was generated according to their correlation with expressions of 4 risk genes respectively, next, GSEA elucidated the significant survival difference between high- and low-expression groups. The expressions level of 4 risk genes served as the phenotype label. The pathways enriched in each phenotype were ranked according to the *P*-value and normalized enrichment score. Top 10 signal pathways were exhibited.

Results

Differentially expressed autophagy-related genes (DEARGs) detection

The GEO dataset (GSE15605 and GSE3189) including the expression profile of 126 specimens (103 SKCM and 23 skin tissues) were selected to identify DEARGs in SKCM. The raw

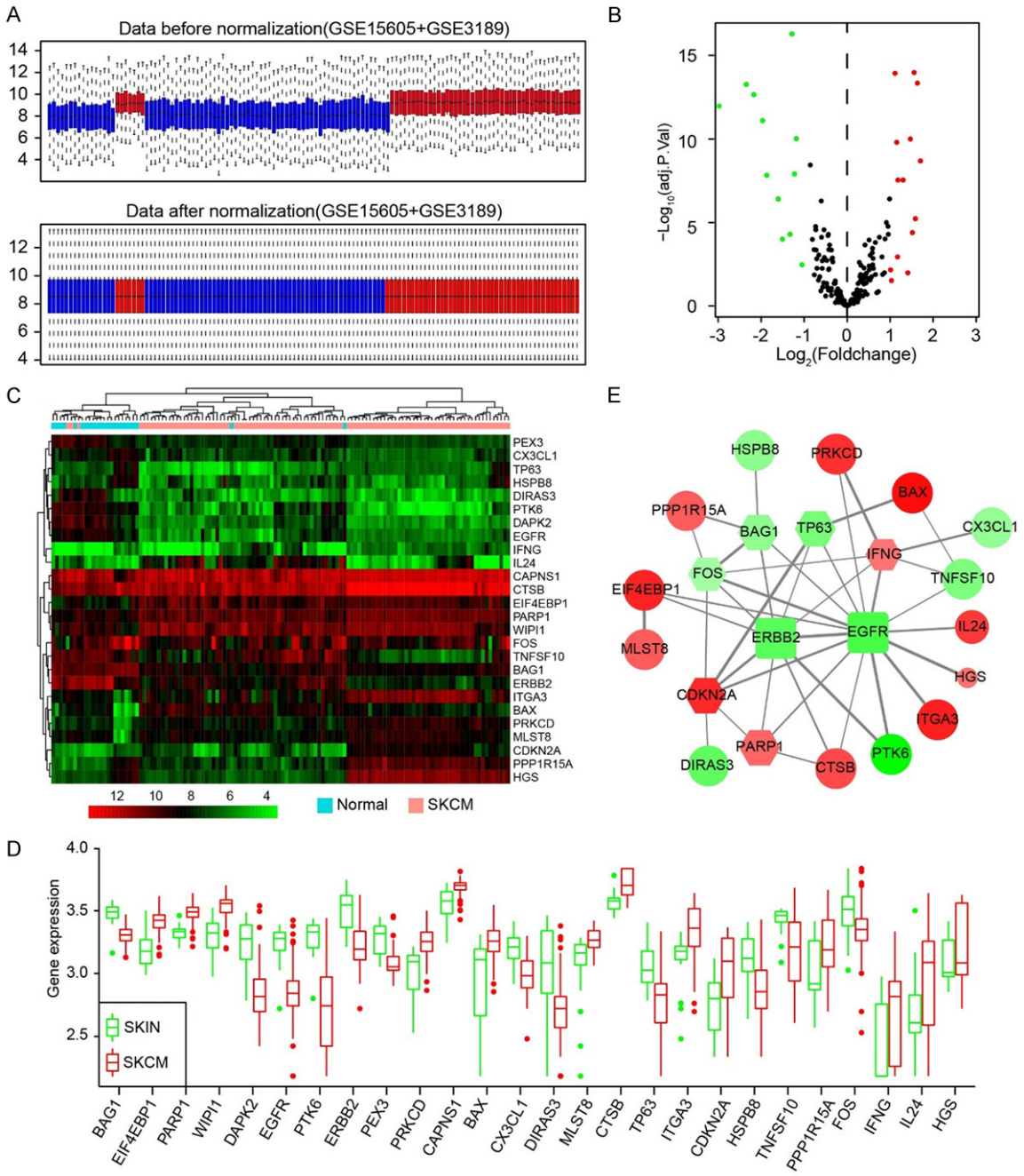

Figure 1. Differentially expressed autophagy-related genes (DEARGs) between 103 SKCM specimens and 23 normal skin tissues. A. Normalization of raw data in GSE15605 and GSE3189 datasets. Blue and red columns represent samples from GSE15605 and GSE3189 datasets respectively. The 23 columns on the left represent normal skin specimens and 103 columns on the right represent SKCM samples. B. Volcano plot of 232 autophagy-related genes (ARGs) in GSE15605 and GSE3189 datasets. Red spots represent up-regulated ARGs, green spots represent down-regulated ARGs. Filter criteria is $|Log_2Fold\ Change| > 1.0$. C, D. Heatmap and boxplot of 26 DEARGs in SKCM and normal tissues. The depth of the color of the columns represents its expression intensity in the corresponding samples. E. PPI network of 26 DEARGs. Red or Green nodes represent up-regulated or down-regulated DEARGs. The depth of the color of the nodes was associated with $log_2Fold\ Change$. There is a negative correlation between *P*-value and nodes' size and a positive correlation between the combined score of protein interaction and ligatures' width. Square and diamond nodes stand for hub genes that interactive with >10 or >4 proteins.

data of 2 GEO datasets were normalized (**Figure 1A**). The horizontal axis represents 126 samples and the vertical axis represents the expression value of all genes. Among the 232

Table 2. All DEARGs, screened between human normal skin tissues and Skin Cutaneous Melanoma (SKCM) tissues with criteria of adjust-*P*-value <0.05 and |log_2Fold Change| >1

Gene	Log_2FC	*P*-value	adjust-*P*-value
BAG1	-1.285	2.69E-19	5.17E-17
EIF4EBP1	1.558	1.10E-16	1.06E-14
PARP1	1.115	1.85E-16	1.18E-14
WIPI1	1.633	9.53E-16	4.57E-14
DAPK2	-2.346	1.43E-15	5.51E-14
EGFR	-2.169	6.95E-15	2.22E-13
PTK6	-3.066	3.90E-14	1.07E-12
ERBB2	-1.966	3.34E-13	8.02E-12
PEX3	-1.184	4.52E-12	9.64E-11
PRKCD	1.470	5.29E-12	1.02E-10
CAPNS1	1.153	9.14E-12	1.59E-10
BAX	1.706	1.30E-10	2.08E-09
CX3CL1	-1.225	9.10E-10	1.25E-08
DIRAS3	-1.868	1.18E-09	1.51E-08
MLST8	1.180	2.46E-09	2.90E-08
CTSB	1.301	2.57E-09	2.90E-08
TP63	-1.601	3.87E-08	3.91E-07
ITGA3	1.587	6.53E-07	5.97E-06
CDKN2A	1.518	5.64E-06	4.01E-05
HSPB8	-1.328	7.92E-06	5.13E-05
TNFSF10	-1.504	1.83E-05	0.0001
PPP1R15A	1.172	0.0003	0.0012
FOS	-1.049	0.0011	0.0034
IFNG	1.009	0.0025	0.0069
IL24	1.412	0.0040	0.0103
HGS	1.031	0.0139	0.0299

ARGs, 26 were differentially expressed in SKCM tissues, including 12 downregulated and 14 upregulated DEARGs. The information of 26 DEARGs was provided in **Table 2**. The volcano map of 232 ARGs was showed in **Figure 1B**. The heatmap (**Figure 1C**) and boxplot (**Figure 1D**) visualized the expression patterns of the 26 DEARGs in SKCM tissues and normal skin tissues. In **Figure 1E**, we constructed a PPI network for 26 DEARGs to exhibit their relationship. Square and diamond shapes present the hub genes with interaction degree >10 or interaction degree >4.

Functional annotation of DEARGs

Functional enrichment analysis was performed on 26 DEARGs. According to the 10 most important GO terms regarding molecular function (MF) and biological processes (BP) categories, DEARGs were potentially involved with positive regulation of cellular protein localization especially protein localization to the membrane, protein tyrosine kinase, or phosphatase binding, and cytokine activity (**Figure 2A**). KEGG enrichment results exhibit that DEARGs were mainly associated with bladder cancer, endocrine resistance and apoptosis (**Figure 2B**).

Establishment of autophagy-related risk model based on the prognostic DEARGs

According to previous results in the paper, there are 26 DEARGs were identified from 2 GEO datasets in total. Then, we sought the prognostic role of 26 DEARGs. The 458 SKCM patients in the TCGA database with complete clinical follow-up data were defined as the training cohort. After combining the expression of all DEARGs with survival data in the training cohort, univariate Cox regression analysis was performed to identify DEARGs related to prognosis, resulting in 8 prognostic DEARGs ($P< 0.05$) (**Figure 3A**). The 8 prognostic DEARGs were candidate genes that were incorporated into the subsequent multivariate Cox regression analysis in the training set, and 4 independent prognostic DEARGs (*CAPNS1*, *DAPK2*, *PARP1* and *PTK6*) were identified to build the predictive risk model (**Figure 3B**). The formula was now obtained to calculate risk scores for each SKCM individuals, risk score = (0.3114 × *CAPNS1* expression) + (-0.4284 × *DAPK2* expression) + (0.3961 × *PARP1*) + (-0.3357 × *PTK6* expression). To establish a quantitative visualization model for SKCM prognosis predicting, 4 prognostic DEARGs were combined to build a nomogram in **Figure 3C**.

Verification of the risk model in TCGA independent cohort and external cohort

The data of 209 SKCM patients from the GSE65904 dataset was an external cohort that was used as the test cohort. We calculated the risk scores for all patients in the training and validation cohorts. According to the training cohort, the median risk score was 1.019. Patients whose risk scores were higher than or less than 1.019 were assigned to the high-risk or low-risk group, respectively. Kaplan-Meier plotter was used to compare the survival outcomes between different risk groups. In the

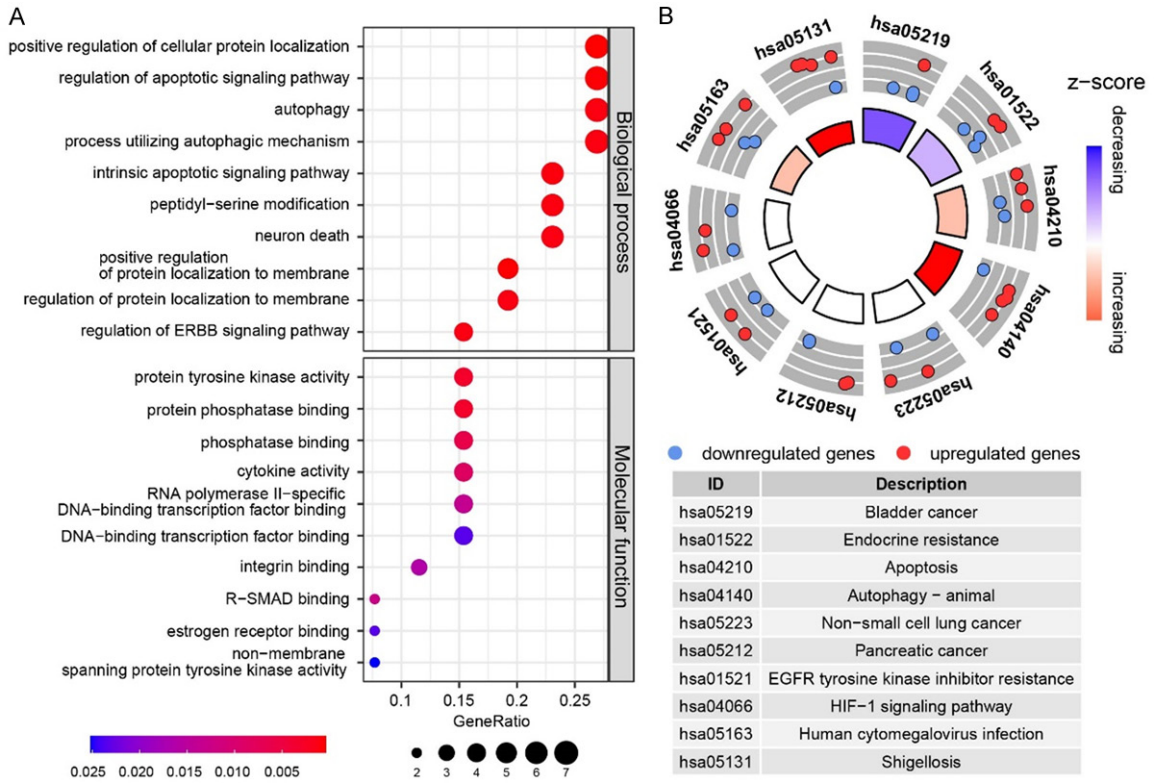

ID	Description
hsa05219	Bladder cancer
hsa01522	Endocrine resistance
hsa04210	Apoptosis
hsa04140	Autophagy − animal
hsa05223	Non−small cell lung cancer
hsa05212	Pancreatic cancer
hsa01521	EGFR tyrosine kinase inhibitor resistance
hsa04066	HIF−1 signaling pathway
hsa05163	Human cytomegalovirus infection
hsa05131	Shigellosis

Figure 2. Functional enrichment analyses of 26 DEARGs. A. Bubble plot of significant GO terms. B. Circle plot of KEGG analyses revealed significant pathways that DEARGs are involved in.

training group and test group, compared to the low-risk group, the survival rate of the high-risk group was significantly lower (**Figure 4A**, **4C**). The ROC curve provided AUC values of all clinical indicators including risk score, to appraise the predictive accuracy of the risk score model. In the training cohort and test cohort, the AUC values for the risk score were 0.788 and 0.627, respectively (**Figure 4B**, **4D**). The accuracy of the risk score to evaluate prognosis was better than other clinical indicators. **Figure 4E-G** displayed the relationship among risk scores, corresponding survival status of patients, and 4 risk genes' expression patterns in the TCGA cohort. Consistent with the training cohort, the mortality of SKCM patients increased as the risk scores increased in the test group (**Figure 4H**, **4I**). We also provided a heatmap to show the expression of 4 risk genes in the GSE65-904 validation set (**Figure 4J**).

Associations of prognostic model and DEARGs with clinicopathological features

Since the TCGA cohort contains relatively complete clinical information of SKCM patients, we evaluated the clinical utility of the prognostic risk model by analyzing the correlation between the risk model and DEARGs with clinical parameters. Risk scores were higher in pathological stage II-IV than in pathological stage 0-I (P = 0.002) (**Figure 5A**), and higher in T classification T3-4 than in T0-2 (P = 2.736e-04) (**Figure 5B**). Because only 11 patients were classified into M1 classification and the M classification of most of the patients were M0, the correlation between risk scores and M classification still needs to explore in the future (**Figure 5C**). The risk score was irrelevant to the N classification of patients (P = 0.363) (**Figure 5D**), although patients classified into the N1-3 classification patients seemed to have a higher risk score than patients classified into the N0 classification. The association between DEARGs that formed the risk score model and clinical characteristics of SKCM patients was also displayed in **Figure 5**.

In **Table 3**, univariate Cox regression revealed that the age, risk score, T/N classification and pathological stage were strongly correlated with survival, whereas, in the multivariate Cox analysis, only risk score and T/N classification were strongly linked to survival. All results

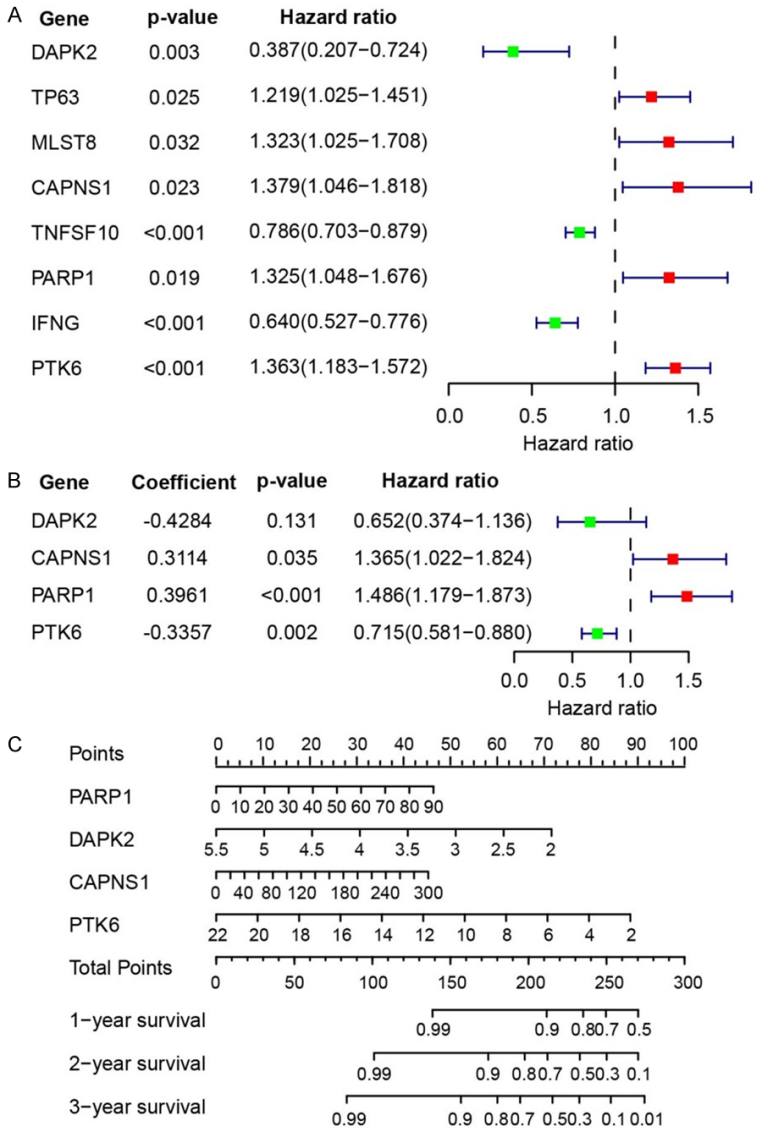

Figure 3. Identify prognostic DEARGs and build a prognostic model based on the TCGA cohort with 458 SKCM patients as the training cohort. A. Forest plots visualized the 8 prognostic DEARGs identified by univariate Cox analysis in the TCGA training cohort. B. Screening of the optimal DEARGs used for the final establishment of the prognostic risk model using multivariate Cox regression analysis. C. The prognostic nomogram for quantitative prediction of SKCM patients' survival.

proved that the autophagy-related risk score model is an independent indicator for the survival prediction of SKCM patients.

Validation of the 4 risk DEARGs included in the risk score model

Kaplan-Meier analysis was used to detect the correlation between the expression of 4 risk DEARGs (*CAPNS1*, *DAPK2*, *PARP1* and *PTK6*) which formed the risk model and OS of SKCM patients. The results exhibited that high expression of *CAPNS1* and *PARP1* was strongly associated with the inferior survival of SKCM patients. Meanwhile, high expression of *DAPK2* or *PTK6* was associated with better OS (**Figure 6A**). We also compared the expression of 4 risk DEARGs (*CAPNS1*, *DAPK2*, *PARP1* and *PTK6*) in SKCM and non-tumor control tissues, according to the results from the oncomine database (**Figure 6B**) and Human Protein Atlas database (**Figure 7A**), *CAPNS1* and *PARP1* were significantly upregulated in SKCM tissues compared with normal skin tissues, and *PTK6* and *DAPK2* were significantly downregulated in SKCM tissues, consistent with their expression patterns in 2 GEO datasets that used to do expression discrepant analysis in **Figure 1**. Immunohistochemistry (IHC) data of DAPK2 is missing in The Human Protein Atlas. In **Figure 7B**, GSEA was applied to identify the pathways enriched in each risk DEARGs in SKCM.

Discussion

Autophagy is a conserved and dynamic self-degradative that is important for cellular homeostasis maintain [20]. A lot of studies had confirmed that the process of autophagy was important in SKCM [21-23]. Multiple pharmaceutical drugs targeting autophagy for cancer treatment had been applied in the clinics [24, 25]. In this paper, we build an autophagy-related risk model for prognosis monitoring for SKCM patients.

The autophagy-related risk model is comprised of 4 genes, including *CAPNS1*, *DAPK2*, *PARP1* and *PTK6*. The risk score model is significantly related to clinicopathological features of SKCM

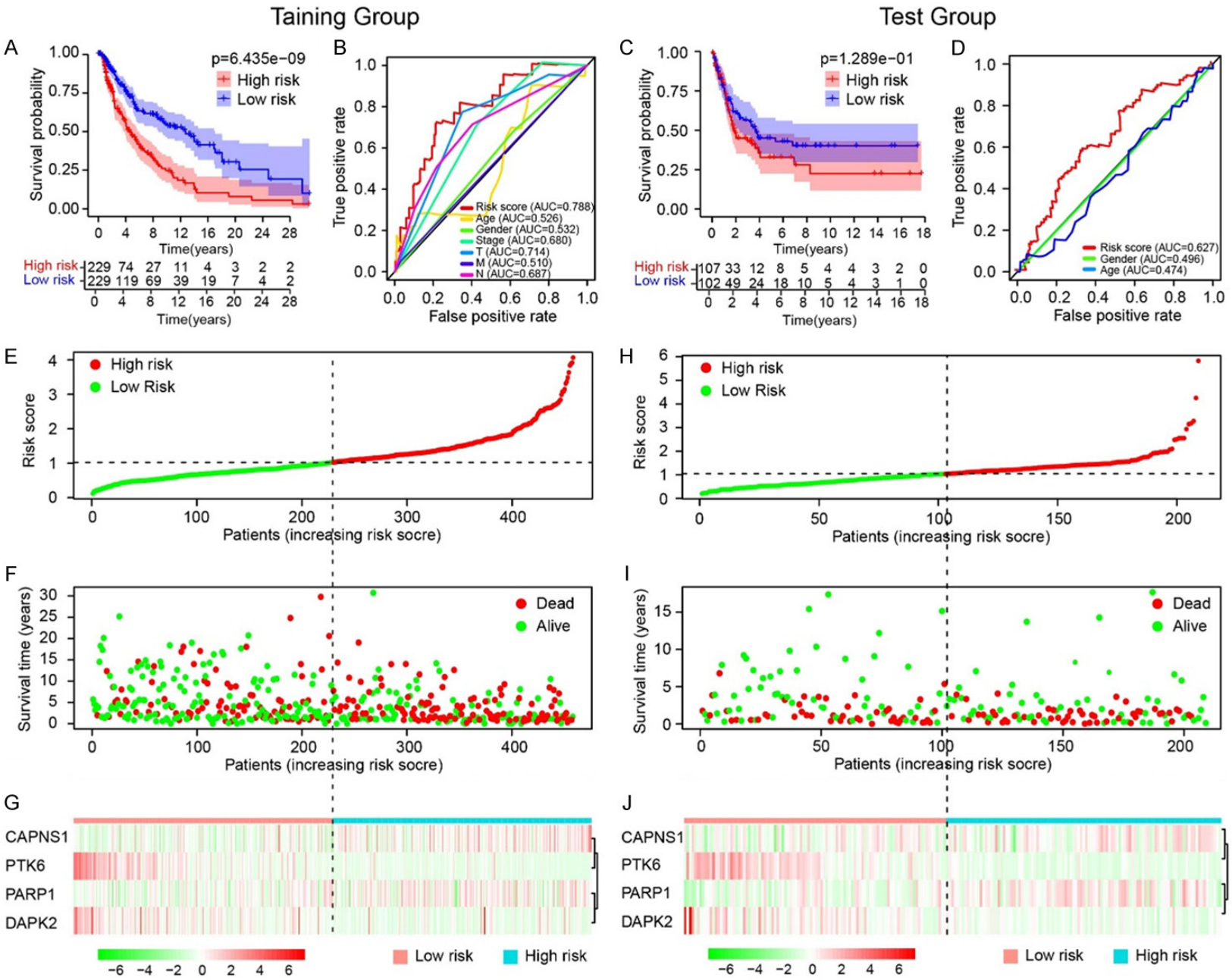
Taining Group
Test Group
A
p=6.435e−09
High risk
Low risk
Survival probability
Time(years)
High risk 229 74 27 11 4 3 2 2
Low risk 229 119 69 39 19 7 4 2
B
True positive rate
False positive rate
Risk score (AUC=0.788)
Age (AUC=0.526)
Gender (AUC=0.532)
Stage (AUC=0.680)
T (AUC=0.714)
M (AUC=0.510)
N (AUC=0.687)
C
p=1.289e−01
High risk 107 33 12 8 5 4 4 3 2 0
Low risk 102 49 24 18 10 5 4 3 1 0
D
Risk score (AUC=0.627)
Gender (AUC=0.496)
Age (AUC=0.474)
E
Risk score
Patients (increasing risk socre)
H
F
Survival time (years)
Dead
Alive
I
G
CAPNS1
PTK6
PARP1
DAPK2
Low risk
High risk
J

Figure 4. Validation of the prognostic risk model in TCGA and GEO independent cohort respectively. A, C. Kaplan-Meier curve of the high-risk and low-risk SKCM patients in the TCGA cohort and GEO cohort. B, D. Survival-dependent ROC curves of risk score and other clinical indicators in the TCGA cohort and GEO cohort. E, F, H, I. risk scores distribution and corresponding survival status of SKCM patients in the TCGA cohort and GEO cohort. G, J. The heatmap of 4 risk genes composed of the risk model in the TCGA cohort and GEO cohort.

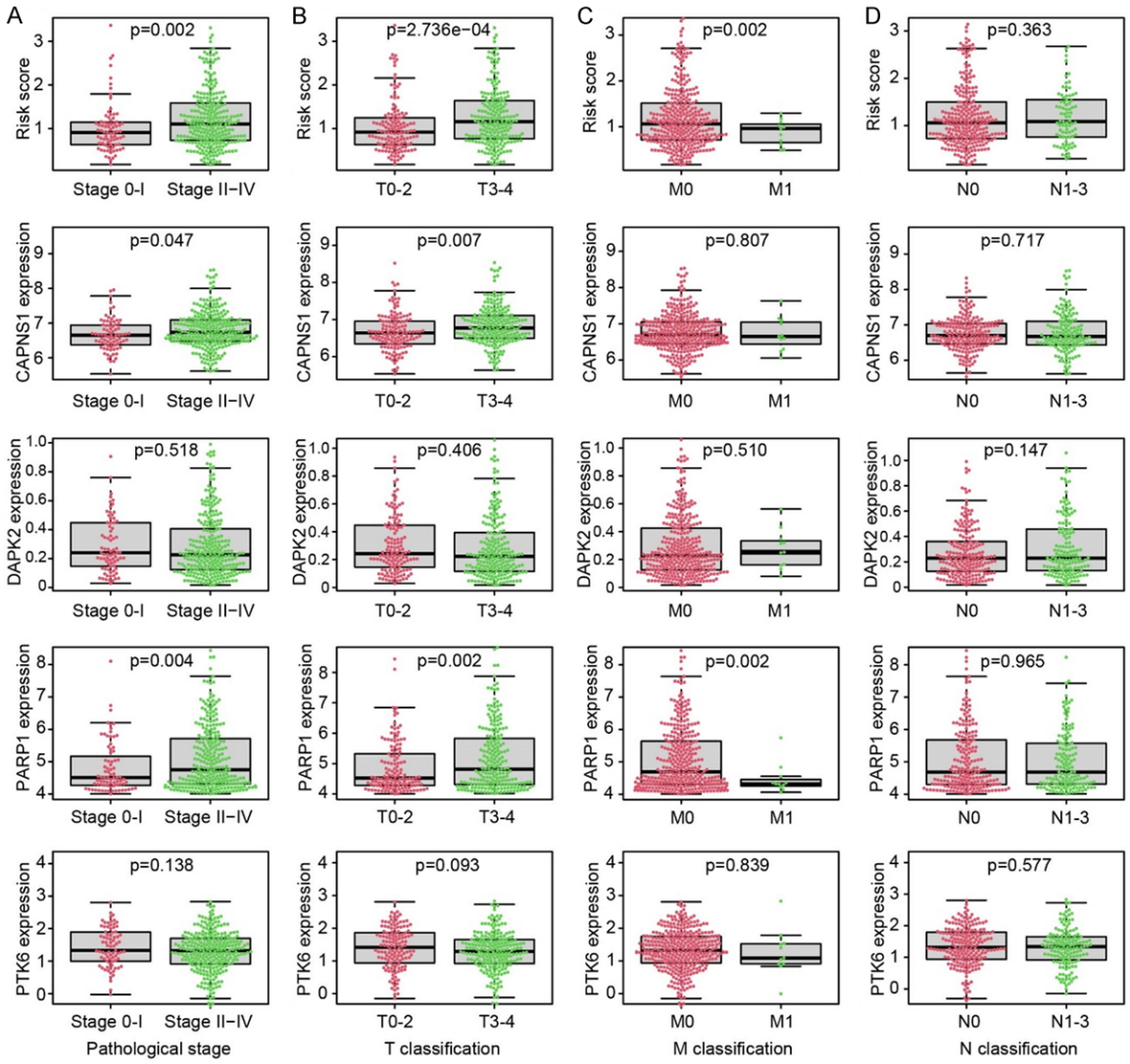

Figure 5. Exploration of clinical correlations between the risk score, 4 risk genes and clinicopathological parameters. A. Pathological stage. B. T classification. C. M classification. D. N classification.

patients. The expression of *CAPNS1* and *PARP1* are significantly correlated with clinicopathological features (especially pathological stage and T classification) of SKCM patients. Several assessment methods in two independent cohorts confirmed that the prognostic signature is an independent indicator for survival predicting and monitoring in SKCM patients. Individual assessment of the prognostic value of 4 genes in SKCM further proved that as DEARGs, the expression trends of these genes in 2 GEO databases are consistent with subsequent verification experiments, and their expression are all correlated with the survival of SKCM patients. Our results confirmed that the risk model built by *CAPNS1*, *DAPK2*, *PARP1* and *PTK6* for prognosis evaluating of SKCM patients is clinically applicable.

CAPNS1 gene also known as CAPN4, encoded the small subunit of the calpain proteases, Enwen *et al.* proved that *CAPNS1* can promote

Table 3. Univariate and multivariate cox regression analyses of risk score and clinicopathologic features in the TCGA group SKCM patients

Variables	Univariate analysis		Multivariate analysis	
	HR (95% CI)	*P*-Value	HR (95% CI)	*P*-Value
RiskScore	1.852 (1.505-2.279)	5.64E-09	1.792 (1.437-2.235)	2.19E-07
Age	1.020 (1.009-1.031)	0.0003	1.010 (0.999-1.021)	0.0863
Gender	1.040 (0.746-1.450)	0.8161	1.016 (0.725-1.424)	0.9253
Pathological Stage	1.402 (1.173-1.676)	0.0002	0.772 (0.562-1.061)	0.1105
T classification	1.386 (1.204-1.597)	5.70E-06	1.384 (1.172-1.633)	0.0001
M classification	1.737 (0.709-4.252)	0.2269	2.046 (0.765-5.475)	0.1540
N classification	1.436 (1.229-1.678)	5.29E-09	1.763 (1.387-2.239)	3.46E-06

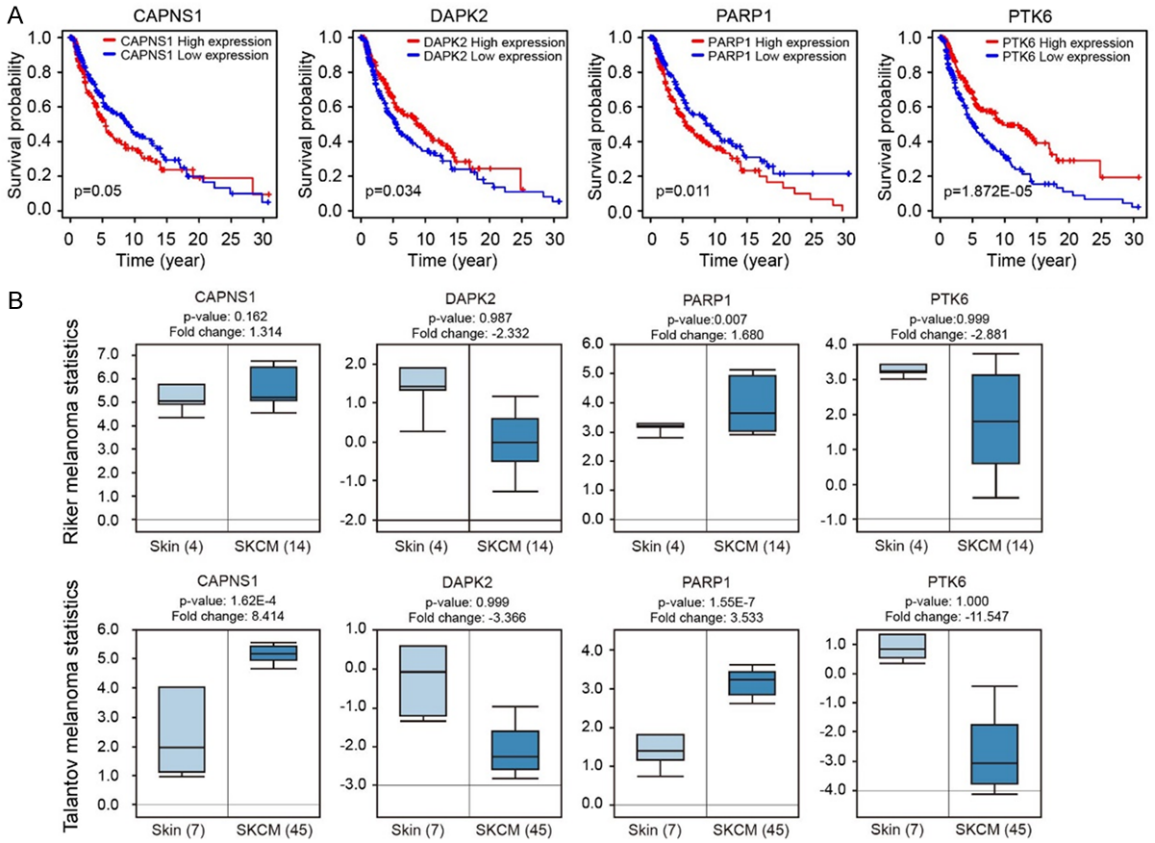

Figure 6. Evaluation of the prognostic value of the 4 risk genes (*CAPNS1*, *DAPK2*, *PARP1* and *PTK6*) that formed the prognostic risk signature. A. Kaplan-Meier analysis of 4 risk genes. B. The mRNA expression levels of 4 risk genes in normal skin and SKCM tissues.

an epithelial-mesenchymal transition to promote SKCM metastasis [26]. Qiao *et al.* reported that increased mRNA expression of *DAPK2* correlated with longer survival in SKCM patients [27]. The nuclear protein PARP1 has been reported can promote invasion and metastasis of distal organs in SKCM cells [28]. We found that researches about the 4 potential prognostic markers and therapeutic targets are still limited now, more work needs to do in the future.

Functional annotation exhibited that 26 DEARGs that we filtered out were mainly involved in various cancers, such as bladder cancer, pancreatic cancer and non-small cell lung cancer. It is generally acknowledged that autophagy had different effects in different stages of

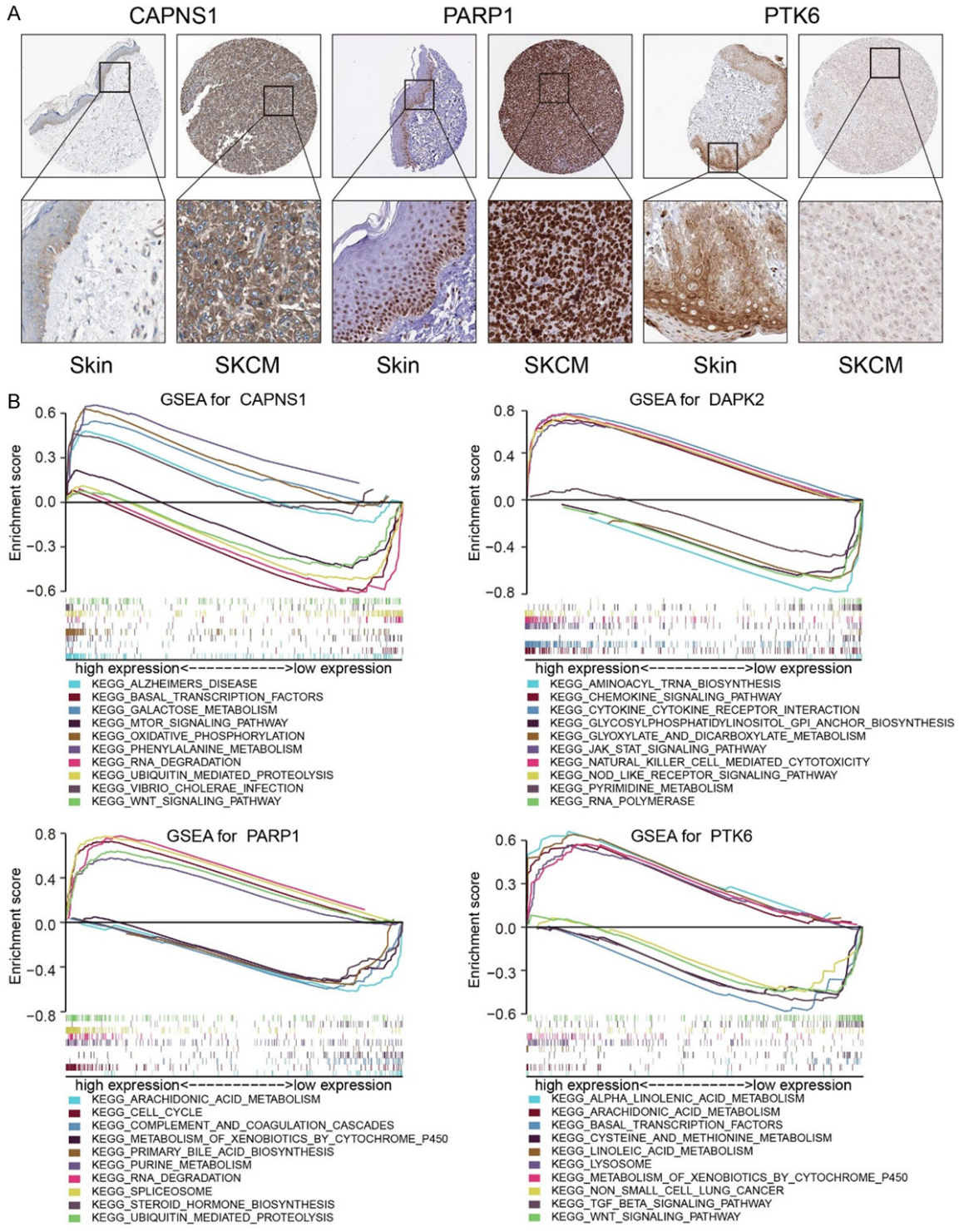

Figure 7. Evaluation of the prognostic value of the 4 risk genes (*CAPNS1*, *DAPK2*, *PARP1* and *PTK6*) at the protein level. A. Immunohistochemistry staining of the 4 risk genes in SKCM and normal tissues. The antibody of *CAPNS1, PARP1, PTK6* protein is HPA006872, HPA045168 and HPA036071. Immunohistochemistry staining result of *DAPK2* is the absence in The Human Protein Atlas database. B. GSEA analysis of 4 risk genes in SKCM.

cancer [29]. Autophagy can promote invasion of cancers in the late stage of the tumor. This suggests that it may be an effective interventional strategy for oncotherapy by autophagy

regulation [30]. Many researchers deemed that the development of more potent and specific autophagy inhibitors for cancer treatment is necessary and promising [31].

Our study established a risk model for survival predicting and prognosis monitoring, we proved it is accurate and reliable with internal validation and external validation in 2 independent cohorts.

Conclusions

Taken together, our work constructed a prognostic risk model with four DEARGs, the model is accurate, and convenient for prognosis monitoring of SKCM patients. It might also benefit for rapid diagnosis, targeted treatment and effective therapeutic intervention.

Acknowledgements

The study was supported by the Nosocomial Scientific Research Fund Projects from the International Peace Maternity and Child Health Hospital of Shanghai Jiao Tong University School of Medicine (No. GFY5801), clinical research special projects from Shanghai Municipal Health Commission (No. 20204Y0230) and Shanghai Sailing Program from Shanghai Science and Technology Committee (No. 19YF1452200).

Disclosure of conflict of interest

None.

Abbreviations

ARGs, Autophagy-related genes; AUC, Area under the curve; BP, Biological Processes; DEARGs, Differentially expressed autophagy-related genes; DEGs, Differentially expressed genes; FDR, False discovery rate; GEO database, Gene Expression Omnibus database; GO, Gene Ontology; GSEA, Gene Set Enrichment Analysis; KEGG, Kyoto Encyclopedia of Genes and Genomes; KM plotter, Kaplan-Meier plotter; $\log_2$FC, $\log_2$Fold Change/Logarithm of Fold Change; MF, Molecular Functions; OS, overall survival; PPI, protein-protein interaction; ROC, Receiver-operator characteristic; SKCM, Skin Cutaneous Melanoma; TCGA, The Cancer Genome Atlas.

Address correspondence to: Dr. Hongjun Fei, Department of Reproductive Genetics, International Peace Maternity and Child Health Hospital, Shanghai Jiao Tong University School of Medicine, No. 910, Hengshan Road, Shanghai 200030, China. Tel: +86-021-64070434; E-mail: feihongjun@alumni.sjtu.edu.cn

References

[1] Bray F, Ferlay J, Soerjomataram I, Siegel RL, Torre LA and Jemal A. Global cancer statistics 2018: GLOBOCAN estimates of incidence and mortality worldwide for 36 cancers in 185 countries. CA Cancer J Clin 2018; 68: 394-424.

[2] Schadendorf D, van Akkooi ACJ, Berking C, Griewank KG, Gutzmer R, Hauschild A, Stang A, Roesch A and Ugurel S. Melanoma. Lancet 2018; 392: 971-984.

[3] Garbe C, Peris K, Hauschild A, Saiag P, Middleton M, Spatz A, Grob JJ, Malvehy J, Newton-Bishop J, Stratigos A, Pehamberger H and Eggermont AM; European Dermatology Forum, European Association of Dermato-Oncology, European Organization of Research and Treatment of Cancer. Diagnosis and treatment of melanoma. European consensus-based interdisciplinary guideline--update 2012. Eur J Cancer 2012; 48: 2375-2390.

[4] Siegel RL, Miller KD, Fuchs HE and Jemal A. Cancer statistics, 2021. CA Cancer J Clin 2021; 71: 7-33.

[5] McKinnon JG, Yu XQ, McCarthy WH and Thompson JF. Prognosis for patients with thin cutaneous melanoma: long-term survival data from New South Wales Central Cancer Registry and the Sydney Melanoma Unit. Cancer 2003; 98: 1223-1231.

[6] Essner R, Lee JH, Wanek LA, Itakura H and Morton DL. Contemporary surgical treatment of advanced-stage melanoma. Arch Surg 2004; 139: 961-966; discussion 966-967.

[7] Sandru A, Voinea S, Panaitescu E and Blidaru A. Survival rates of patients with metastatic malignant melanoma. J Med Life 2014; 7: 572-576.

[8] Miller R, Walker S, Shui I, Brandtmuller A, Cadwell K and Scherrer E. Epidemiology and survival outcomes in stages II and III cutaneous melanoma: a systematic review. Melanoma Manag 2020; 7: MMT39.

[9] Ferguson PM, Gershenwald JE and Scolyer RA. Staging of cutaneous melanoma: is there room for further improvement? JAMA Netw Open 2018; 1: e180086.

[10] Gutiérrez García-Rodrigo C, Antonini A, Rocco T, Pellegrini C, Micantonio T and Fargnoli MC.

Staging and follow-up of cutaneous melanoma patients. G Ital Dermatol Venereol 2017; 152: 231-240.
[11] Keung EZ and Gershenwald JE. The eighth edition American Joint Committee on Cancer (AJCC) melanoma staging system: implications for melanoma treatment and care. Expert Rev Anticancer Ther 2018; 18: 775-784.
[12] Gerami P, Busam K, Cochran A, Cook MG, Duncan LM, Elder DE, Fullen DR, Guitart J, LeBoit PE, Mihm MC Jr, Prieto VG, Rabkin MS, Scolyer RA, Xu X, Yun SJ, Obregon R, Yazdan P, Cooper C, Weitner BB, Rademaker A and Barnhill RL. Histomorphologic assessment and interobserver diagnostic reproducibility of atypical spitzoid melanocytic neoplasms with long-term follow-up. Am J Surg Pathol 2014; 38: 934-940.
[13] Davis LE, Shalin SC and Tackett AJ. Current state of melanoma diagnosis and treatment. Cancer Biol Ther 2019; 20: 1366-1379.
[14] Farmer ER, Gonin R and Hanna MP. Discordance in the histopathologic diagnosis of melanoma and melanocytic nevi between expert pathologists. Hum Pathol 1996; 27: 528-531.
[15] McGinnis KS, Lessin SR, Elder DE, Guerry D 4th, Schuchter L, Ming M and Elenitsas R. Pathology review of cases presenting to a multidisciplinary pigmented lesion clinic. Arch Dermatol 2002; 138: 617-621.
[16] Troxel DB. Pitfalls in the diagnosis of malignant melanoma: findings of a risk management panel study. Am J Surg Pathol 2003; 27: 1278-1283.
[17] Mizushima N and Komatsu M. Autophagy: renovation of cells and tissues. Cell 2011; 147: 728-741.
[18] Ndoye A and Weeraratna AT. Autophagy-an emerging target for melanoma therapy. F1000Res 2016; 5: F1000 Faculty Rev-1888.
[19] Di Leo L, Bodemeyer V and De Zio D. The complex role of autophagy in melanoma evolution: new perspectives from mouse models. Front Oncol 2019; 9: 1506.
[20] Klionsky DJ and Emr SD. Autophagy as a regulated pathway of cellular degradation. Science 2000; 290: 1717-1721.
[21] Lazova R, Klump V and Pawelek J. Autophagy in cutaneous malignant melanoma. J Cutan Pathol 2010; 37: 256-268.
[22] Mgrditchian T, Arakelian T, Paggetti J, Noman MZ, Viry E, Moussay E, Van Moer K, Kreis S, Guerin C, Buart S, Robert C, Borg C, Vielh P, Chouaib S, Berchem G and Janji B. Targeting autophagy inhibits melanoma growth by enhancing NK cells infiltration in a CCL5-dependent manner. Proc Natl Acad Sci U S A 2017; 114: E9271-E9279.
[23] Tang DY, Ellis RA and Lovat PE. Prognostic impact of autophagy biomarkers for cutaneous melanoma. Front Oncol 2016; 6: 236.
[24] Perez-Hernandez M, Arias A, Martinez-Garcia D, Perez-Tomas R, Quesada R and Soto-Cerrato V. Targeting autophagy for cancer treatment and tumor chemosensitization. Cancers (Basel) 2019; 11: 1599.
[25] Yoshida GJ. Therapeutic strategies of drug repositioning targeting autophagy to induce cancer cell death: from pathophysiology to treatment. J Hematol Oncol 2017; 10: 67.
[26] Wang EW, Wang DL, Li B, Ma HW, Wang CM, Guan LL, Zhang HW, Yi L and Li SL. Capn4 promotes epithelial-mesenchymal transition in human melanoma cells through activation of the Wnt/beta-catenin pathway. Oncol Rep 2017; 37: 379-387.
[27] Li Q, Zhang LY, Wu S, Huang C, Liu J, Wang P and Cao Y. Bioinformatics analysis identifies MicroRNAs and target genes associated with prognosis in patients with melanoma. Med Sci Monit 2019; 25: 7784-7794.
[28] Rodriguez MI, Peralta-Leal A, O'Valle F, Rodriguez-Vargas JM, Gonzalez-Flores A, Majuelos-Melguizo J, Lopez L, Serrano S, de Herreros AG, Rodriguez-Manzaneque JC, Fernandez R, del Moral RG, de Almodovar JM and Oliver FJ. PARP-1 regulates metastatic melanoma through modulation of vimentin-induced malignant transformation. PLoS Genet 2013; 9: e1003531.
[29] Mulcahy Levy JM and Thorburn A. Autophagy in cancer: moving from understanding mechanism to improving therapy responses in patients. Cell Death Differ 2020; 27: 843-857.
[30] Li X, He S and Ma B. Autophagy and autophagy-related proteins in cancer. Mol Cancer 2020; 19: 12.
[31] Amaravadi RK, Kimmelman AC and Debnath J. Targeting autophagy in cancer: recent advances and future directions. Cancer Discov 2019; 9: 1167-1181.